The visible and hidden climatic effects on Earth's denudation

I. Vergara, F. Santibañez, R. Garreaud, G. Aguilar

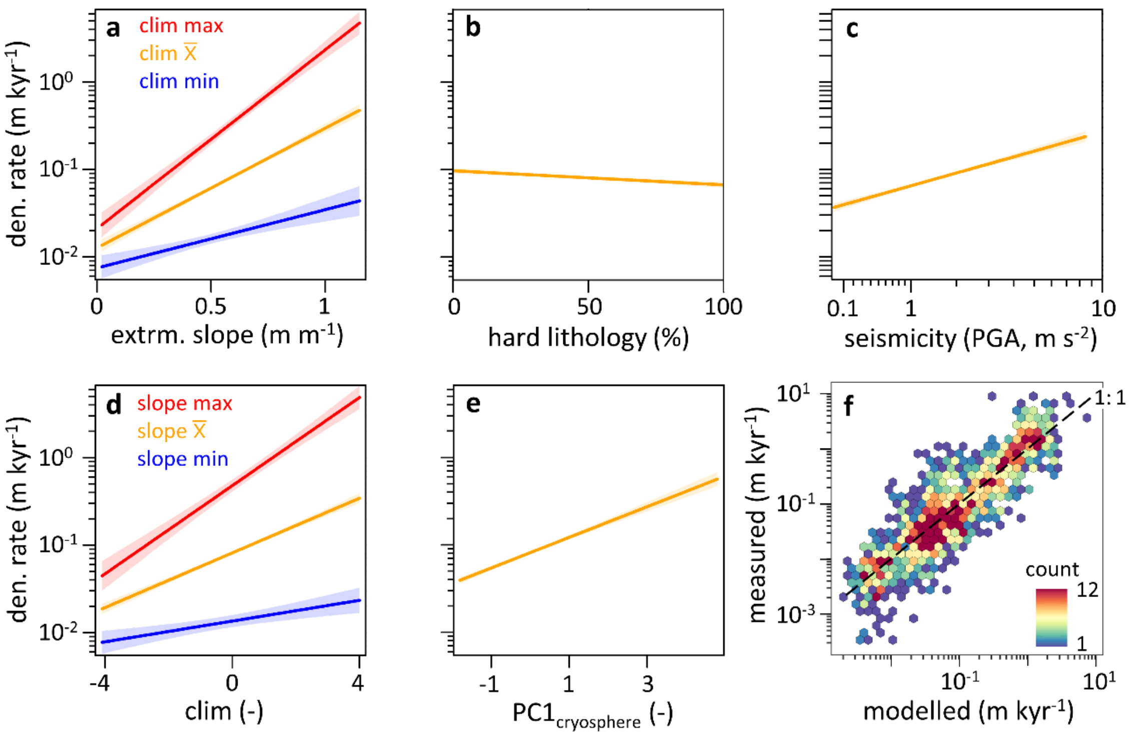

Figure S1. (*a*-*e*) Partial effects of the five covariates in the main regression model (Table S2). Orange lines indicate predicted fits as a function of x-axis covariate and fixing the others at their averages. For (*a*) and (*d*), the *clim* and *slope* covariates are also fixed at their minima (blue) and maxima (red) to show their interaction. (*f*) Measured vs. modelled denudation.

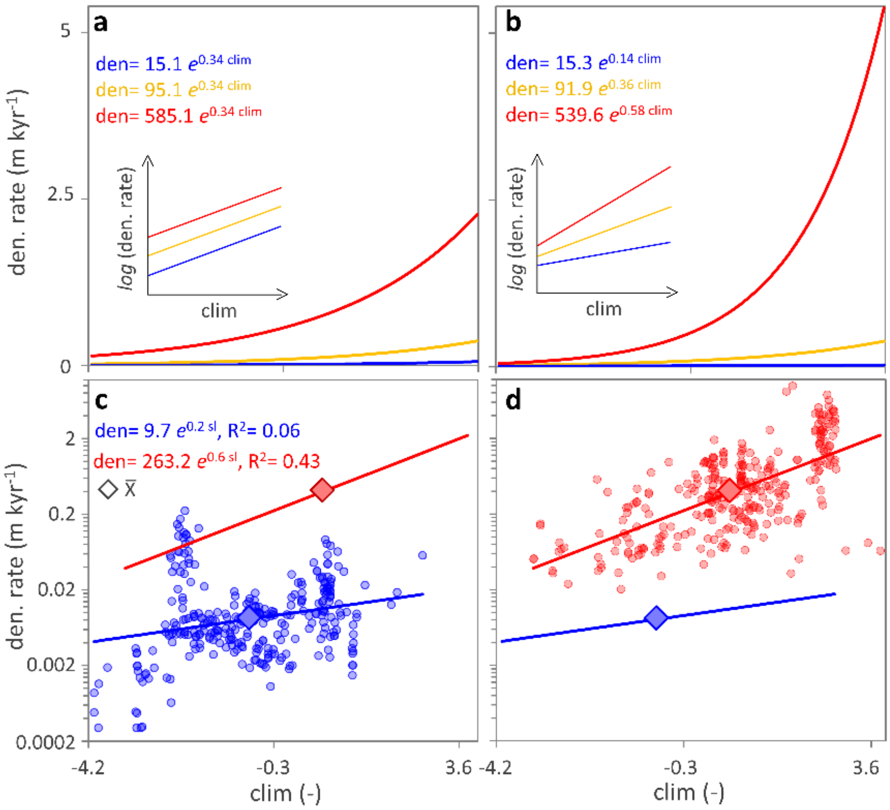

Figure S2. Similar to Fig. 2, but the roles of *slope* and *clim* are reversed.

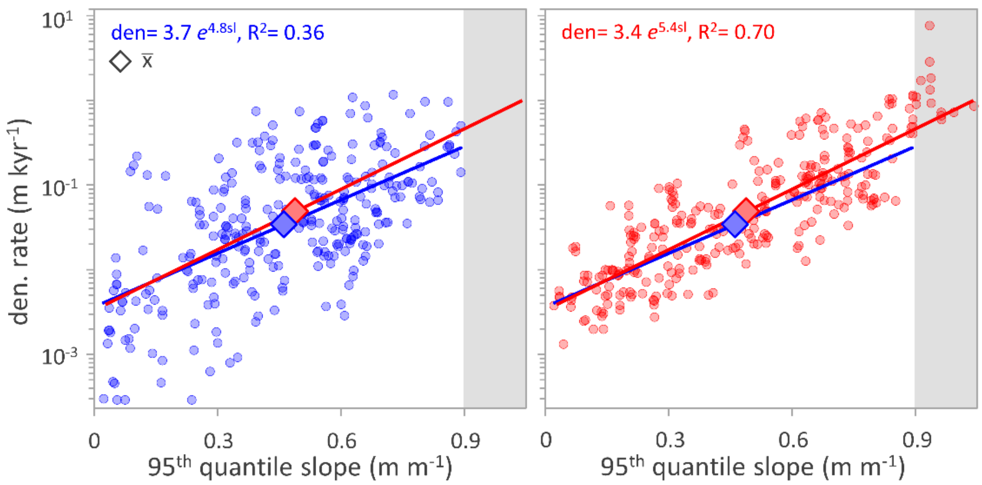

Figure S3. Similar to Fig. 2c,d, but basin selection was made according to the extreme streamflow variable (Qmax_ln in Table S9). The difference between the slopes of the fits is higher for the covariate *clim* (Fig. 2c,d), reflecting the greater importance of the hillslope processes discussed in the main text.

Table S1. Main results of the regression model selected for the dataset without basins with a lot of solid precipitation or glacial volume.

dependent variable	R^2	adjusted R^2	AIC	*p*-value	coefficient	coefficient estimate
ln (den)	71.8	71.6	3,802.7	$<2.2 \cdot 10^{-16}$	intercept	-4.37
					hard	-0.004
					ln (PGA+0.1)	0.44
					ln (A-100)	-0.02
					ln (FCF+100)	0.99
					ln (pPP+1,000)	0.25
					sl_95	-3.98
					sl_95 · *ln* (pPP+1,000)	1.05

Note. All coefficients are significant at 0.001 level, except the area (paleo-precipitation), which is significant at 0.05 (0.01) level. *ln* means natural logarithm. Go to Table S13 to know the variables used in the model selection and to Table S10 for the meaning of variables abbreviation. Although the slope has a negative coefficient, its effect is positive for any paleo-precipitation value in the database due to the high value of the interactive effect's coefficient.

Table S2. Main results of the regression model selected.

dependent variable	R^2	adjusted R^2	AIC	*p*-value	coefficient	coefficient estimate
ln (den)	78.7	78.6	4,510.6	$<2.2 \cdot 10^{-16}$	intercept	1.91
					hard	-0.004
					ln (PGA+1)	0.83
					$PC1_{cry}$	0.40
					clim	0.13
					sl_95	3.15
					sl_95 · clim	0.39

Note. All coefficients are significant at 0.001 level. *ln* means natural logarithm. Go to Table S12 to know the variables used in the model selection and to Table S9 for the meaning of variables abbreviation.

Table S3. Metrics of the regressions *ln* (den) = *m* sl_95 + *b*. Subgroups were obtained for samples of 200, 300 (Fig. 2c,d) and 400 basins and according to the variables *Qmax_ln* and *clim*.

basins number	variable	subgroup	R^2	fit slope -*m*- [$\bar{X}$ H – $\bar{X}$ L]	*ln* (den) [$\bar{X}$ H – $\bar{X}$ L]	sl_95 [$\bar{X}$ H – $\bar{X}$ L]
200	*Qmax_ln*	highest lowest	0.69 0.39	0.04	0.59	0.05
	clim	highest lowest	0.60 0.33	3.27	2.45	0.22
300	*Qmax_ln*	highest lowest	0.70 0.36	0.62	0.35	0.03
	clim	highest lowest	0.64 0.33	3.33	1.91	0.19
400	*Qmax_ln*	highest lowest	0.69 0.39	0.79	0.34	0.03
	clim	highest lowest	0.63 0.37	2.71	1.56	0.15

Note. H (L) means highest (lowest). Go to Table S9 to know the meaning of variables abbreviation.

Table S4. Main results of the regression model selected including only topographic and bioclimatic variables associated with fluvial erosion.

dependent variable	R^2	adjusted R^2	AIC	*p*-value	coefficient	coefficient estimate
ln (den)	68.3	68.2	5,177.3	$<2.2 \cdot 10^{-16}$	intercept	1.16
					hard	-0.003
					ln (PGA+1)	0.70
					ln (SWE+10)	0.27
					K_{sn}_vz	0.03

Note. All coefficients are significant at 0.001 level. *ln* means natural logarithm. Go to Table S12 to know the variables used in the model selection and to Table S9 for the meaning of variables abbreviation.

Table S5. Main results of the selected regression model by replacing slope variables with a resolution of 3 arc-second by those with a resolution of 15 arc-second.

dependent variable	R^2	adjusted R^2	AIC	*p*-value	coefficient	coefficient estimate
ln (den)	77.5	77.4	4,603	$<2.2 \cdot 10^{-16}$	intercept	2.52
					hard	-0.005
					ln (PGA+1)	0.92
					ln (A-100)	-0.02
					$PC1_{cry}$	0.41
					clim	0.21
					sl_95_15s	3.70
					sl_95_15s · clim	0.48

Note. All coefficients are significant at 0.001 level, expect the area, which is significant at 0.05 level. *ln* means natural logarithm. Go to Table S12 to know the variables used in the model selection and to Table S9 for the meaning of variables abbreviation.

Table S6. Main results of the regression model selected to predict average slope (sl).

dependent variable	**R^2**	**adjusted R^2**	**AIC**	***p*-value**	**coefficient**	**coefficient estimate**
ln (sl + 0.4)	73.3	73.2	-1,820.1	$<2.2 \cdot 10^{-16}$	intercept	-2.33
					ln (soft +1)	-0.02
					ln (PGA2475+0.1)	0.1
					$PC1_{cry}$	0.06
					ln (int_daily)	0.23
					ln (elev+100)	0.13

Note. All coefficients are significant at 0.001 level. *ln* means natural logarithm. Go to Table S12 to know the variables used in the model selection and to Table S9 for the meaning of variables abbreviation.

Table S7. Main results of the regression model selected to predict the 95th quantile slope (sl_95).

dependent variable	**R^2**	**adjusted R^2**	**AIC**	***p*-value**	**coefficient**	**coefficient estimate**
ln (5 - sl_95)	74.2	74.1	-6.818,0	$<2.2 \cdot 10^{-16}$	intercept	1.90
					litho	0.001
					ln (PGA2475+0.1)	-0.02
					$PC1_{cry}$	-0.02
					ln (int_daily)	-0.05
					ln (elev+100)	-0.03

Note. All coefficients are significant at 0.001 level. *ln* means natural logarithm. Coefficients' symbols are inverse to what should be expected because the dependent variable was inverted when the logarithm was applied (if the real value of the dependent variable is recovered, covariates' effects take the correct direction). Go to Table S12 to know the variables used in the model selection and to Table S9 for the meaning of variables abbreviation.

Table S8. C-factor values assigned to the land cover types of Bicheron et al. (2011) based on the works of Ortíz-Rodríguez et al. (2019) and Borselli et al. (2008) (and references therein).

value	land cover	C-factor
11	Post-flooding or irrigated croplands (or aquatic)	0.1
14	Rainfed croplands	0.15
20	Mosaic cropland (50-70%) / vegetation (grassland/shrubland/forest) (20-50%)	0.15
30	Mosaic vegetation (grassland/shrubland/forest) (50-70%) / cropland (20-50%)	0.1
40	Closed to open (>15%) broadleaved evergreen or semi-deciduous forest (>5m)	0.05
50	Closed (>40%) broadleaved deciduous forest (>5m)	0.004
60	Open (15-40%) broadleaved deciduous forest/woodland (>5m)	0.05
70	Closed (>40%) needleleaved evergreen forest (>5m)	0.004
90	Open (15-40%) needleleaved deciduous or evergreen forest (>5m)	0.05
100	Closed to open (>15%) mixed broadleaved and needleleaved forest (>5m)	0.05
110	Mosaic forest or shrubland (50-70%) / grassland (20-50%)	0.05
120	Mosaic grassland (50-70%) / forest or shrubland (20-50%)	0.1
130	Closed to open (>15%) (broadleaved or needleleaved, evergreen or deciduous) shrubland (<5m)	0.1
140	Closed to open (>15%) herbaceous vegetation (grassland, savannas or lichens/mosses)	0.13
150	Sparse (<15%) vegetation	0.15
160	Closed to open (>15%) broadleaved forest regularly flooded (semi-permanently or temporarily) - Fresh or brackish water	0.004
170	Closed (>40%) broadleaved forest or shrubland permanently flooded - Saline or brackish water	0.004
180	Closed to open (>15%) grassland or woody vegetation on regularly flooded or waterlogged soil - Fresh, brackish or saline water	0.1
190	Artificial surfaces and associated areas (Urban areas >50%)	0.001
200	Bare areas	0.6
210	Water bodies	0
220	Permanent snow and ice	0.01
230	No data (burnt areas, clouds)	NA

Supplementary Text

<u>Supplementary Discussion</u>

Vegetation effects

The negative effects of vegetation on denudation are: runoff obstruction (Schmid et al., 2018), decreased surface and soil water content through evapotranspiration, dampened rain intensity, and enlarged soil cohesion caused by root anchorage (Vergani et al., 2017). Instead, positive effects are increased soil surcharge (Vorpahl et al. 2013), rock breakage by root growth (Porder, 2019), increased soil hydraulic conductivity because of root networks (Qin et al., 2022), and increased weathering (Perron, 2017). As also mentioned in the main text, this last effect has positive feedback with erosion, because it decreases rock strength, which increases erosion, which in turn exposes new fresh rock surfaces to be weathered.

<u>Supplementary Methods</u>

Dataset with non-cryoshperic basins

The basins dataset excluding those with a lot of solid precipitation or glaciers was generated filtering basins with average snow water equivalent ≥ 1,500mm yr^{-1} or glacier volume per area ≥ 500.000m^3 km^{-2} (volume data downloaded from Farinotti et al. (2019)). To set glacier threshold, it was used as a reference the value of a basin where we know that its fluvial sediment discharge has a glacial component (S094WTS014 of Table S9; Aconcagua River basin; 542.000m^3 km^{-2}).

Fluvial erosion model

The model including only topographic and climatic variables associated with fluvial erosion (Table S3) was carried out with the variables indicated in Table S12. The 9% difference of this model with one without restrictions was calculated using the selected model for slope variables with 15 arc-second resolution to eliminate any difference associated with data resolution (Table S4).

Fluvial area

To estimate basins' area covered by rivers (Discussion section), firstly, for each basin it was removed the area with an annual average temperature less than 1°C (https://www.worldclim.org/data/index.html), which would be where periglacial and glacial processes represent the largest fraction of denudation (Tapia Baldis et al., 2019). Then, it was multiplied the length of every river reach with its width modelled for high streamflow conditions (see Topography subsection in the main text). Finally, surfaces of each river reach of each basin were added and this value was divided by basin area. In the main text are indicated the minimum and maximum values.

Maximum effect of bioclimatic condition

The uncertainty of the maximum denudation variation depending on bioclimatic condition (Discussion section) was calculated using the 95% confidence intervals of Figure S1a. The maximum expected variation was calculated by subtracting the value of the lower confidence interval of the slope effect for minimum *clim* from the upper confidence interval value of the slope effect for maximum *clim*. In contrary way, the minimum expected variation was calculated by subtracting the value of the upper confidence interval of the slope effect for minimum *clim* from the lower confidence interval value of the slope effect for maximum *clim*. The expected variation of 38 times was calculated assuming a maximum 95th quantile slope in hyper-arid setting of 0.82m m^{-1}, while the expected variation of 109 times was calculated assuming a maximum 95th quantile slope in hyper-arid setting of 1.15m m^{-1}.

Slope models building

An automatic model selection was also used to predict basins slopes (Tables S6 and S7), but the Topography group was discarded and mean basin elevation was included as a candidate covariate (Tables S12 and S15). Lithology was used because the harder the rocky outcrops, the more it can withstand high slopes (Ward et al., 2012). Glaciers are efficient at shaping landscape and generating steep valleys. Seismicity was interpreted as a proxy of uplift over the past thousands or tens of thousands of years. Finally, elevation was used to represent uplift over longer periods and normalize topographic dynamics of basins. To avoid predicting negative slope values, logarithms of the mean and 95th quantile slope were used, even though they do not have high skewness.

Bibliography

Farinotti, D., et al. 2019. A consensus estimate for the ice thickness distribution of all glaciers on Earth. *Nature Geoscience*, *12*(3), 168–173. https://doi.org/10.1038/s41561-019-0300-3

Granger, D.E., Schaller, M. 2014. Cosmogenic nuclides and erosion at the watershed scale. *Elements*, 10(5), 369–373. https://doi.org/10.2113/gselements.10.5.369

Ortíz-Rodríguez, A.J., Muñoz-Robles, C., Borselli, L. 2019. Changes in connectivity and hydrological efficiency following wildland fires in Sierra Madre Oriental, Mexico. *Science of the Total Environment*, 655, 112–128. https://doi.org/10.1016/j.scitotenv.2018.11.236

Qin, M., et al. 2022. Occurrence of shallow landslides triggered by increased hydraulic conductivity due to tree roots. *Landslides*, 19(11), 2593–2604. https://doi.org/10.1007/s10346-022- 664 01921-8

Tapia Baldis, C., D. Trombotto Liaudat, A. Ahumada. 2019. Ambiente periglacial y regiones geocriológicas en los Andes de San Juan (28°-33°S). *Revista de la Asociación Geológica Argentina,* 76, 46–63. https://revista.geologica.org.ar/raga/article/view/130

Vorpahl, P., Dislich, C., Elsenbeer, H., Märker, M., Schröder, B. 2013. Biotic controls on shallow translational landslides. *Earth Surface Processes and Landforms*, 38, 198–212. https://doi.org/10.1002/esp.3320

Ward, D.J., Anderson R.S., Haeussler P.J. 2012. Scaling the Teflon Peaks: Rock type and the generation of extreme relief in the glaciated western Alaska Range, J. Geophys. Res. Earth Surf., 117, F01031. 10.1029/2011JF002068